AIAA-2001-1162
Reduction of Tunnel Dynamics at the National Transonic Facility (Invited)

W. A. Kilgore, S. Balakrishna, and D. H. Butler
NASA Langley Research Center
Hampton, Virginia

39th AIAA Aerospace Sciences Meeting & Exhibit
8-11 January 2001
Reno, Nevada

AIAA-2001-1162

REDUCTION OF TUNNEL DYNAMICS AT THE NATIONAL TRANSONIC FACILITY

W. A. Kilgore*, S. Balakrishna‡, and D. H. Butler†
Aerodynamics, Aerothermodynamics, and Acoustics Competency
NASA Langley Research Center
Hampton, Virginia

ABSTRACT

This paper describes the results of recent efforts to reduce the tunnel dynamics at the National Transonic Facility. The results presented describe the findings of an extensive data analysis, the proposed solutions to reduce dynamics and the results of implementing these solutions. These results show a 90% reduction in the dynamics around the model support structure and a small impact on reducing model dynamics. Also presented are several continuing efforts to further reduce dynamics.

INTRODUCTION

The National Transonic Facility (NTF) is the first large scale closed circuit fan drive cryogenic pressure tunnel designed to provide flight Reynolds number testing at transonic conditions in a ground based facility. Throughout the NTF's history several testing programs were cut short, or severely limited, because of dynamics. These limitations manifest themselves as excessive balance dynamic loads, large model displacements and increased data scatter.

Excessive model and/or tunnel movements (i.e. dynamics) can produce questionable results and concern over the safety of the model, instrumentation and the facility. Because the NTF is capable of generating large dynamic pressures (up to 7000psf) and high Reynolds numbers (up to 146million/ft) the dynamics are greatly amplified. Figure 1 shows the NTF operational envelope.

Several efforts to understand and minimize the dynamics were conducted and documented over the history of the NTF.[1,2,3,4] These efforts had limited opportunity to implement any proposed solutions. In FY-2000 a concentrated effort was established to "take action" and implement several solutions. The results of this effort are presented in this paper.

NOMENCLATURE

A	Area
ã	measured fluctuating acceleration, (RMS)
M	Mach number
P_T	tunnel total pressure
p′	measured fluctuating pressure, (RMS)
q	dynamic pressure
Re	Reynolds number in million/chord
t	time, s
T	tunnel flow total temperature

Subscripts and Abbreviations

X	axial direction, tunnel flow axis
Y	lateral direction, orthogonal to X and Z
Z	vertical direction, orthogonal to X and Y
AF	balance axial force
ARC	arc sector
DSSF	down stream support frame
FF	fixed fairing
HSD	high-speed diffuser
MSF	model support frame
NF	balance normal force
PM	balance pitching moment
RM	balance roll moment
RMS	root mean square
SF	balance side force
TS	test section
YM	balance yaw moment

NTF STRUCTURE

The NTF dynamics can be easily divided in to three separate areas (internal support structure, model support structure and model/balance/sting structure). Each area has its own unique

* Dynamics and Control Engineer, Research Facilities Branch, Senior Member, AIAA

‡ Senior Research Scientist, ViGYAN Inc.

† Senior Design Engineer, ViGYAN Inc.

dynamics, and when the dynamics in one area coalesce with another area, excessive dynamics occur.

Internal Support Structure

Because the NTF is a cryogenic pressure tunnel, several unique features are inherent in its design to accommodate the large changes in temperatures (150°F to –250°F) that preclude any fixed mountings or supports. These unique features are most prevalent in the area of the internal support structure for the test section. Figure 2 shows the original build-up of the NTF test section outside the plenum and indicates the support points and the direction of constraint.

Unique to the NTF, the entire test section support structure is free to move; and constrained vertically and laterally using pads and guides between the test section and the plenum pressure shell as shown in figure 3. The upstream and downstream portions of the test section are separate and independently secured with accommodations for movement via Bellevilles spring washers at the front and back of the plenum bulkheads.

Model Support and Model/Balance/Stings Structure

The model support system is mounted within the test section support structure as shown in figure 4. The model is supported on the end of a 13ft sting and attaches to the roll drive that is installed in the arc sector. The entire arc sector, roll drive, sting and model (+35000lbs) rotates to pitch the model assembly.

The arc sector rides between four I-beams as shown in figures 2 and 5 (one set of four on top and one set of four on the bottom). These I-beams connect between the down-stream support frame (DSSF) and the model support frame (MSF) providing stiffness to the model support structure.

The arc sector maintains its alignment and load carrying capability through four sets of lateral bearings (two upper pairs and two lower pairs) and two thrust bearings (one upper unit and one lower unit) as shown in figure 4. These bearings are mounted just below the innermost I-beams adjacent to the arc sector. Each bearing provides a sliding surface on the arc sector that is spring loaded to 2000lbs with Bellevilles washers. All the loads generated from testing are distributed through the bearings into the I-beams, DSSF and MSF. As shown in figure 2, the DSSF is constrained vertically and laterally, while the MSF is cantilevered off the DSSF with no direct constraints.

Immediately behind the arc sector is a fixed fairing (does not move with the arc sector) as shown in figure 4. The fixed fairing is a hollow aero-faring that consists of horizontal flow liner panels connected to a solid vertical beam at the aft end of the fixed fairing and extends forward to the aft edge of the arc sector. This fixed fairing vertical beam spans the test section, is secured to the ceiling, and passes down through the floor for several feet to where it is vertically pinned.

ANALYSIS

An extensive amount of dynamic data was collected over several test programs covering the entire operational envelope of the tunnel. This data included 128 channels (sampled at 320 samples/second, simultaneous sample and hold) of accelerations, positions, loads and fluctuating pressures located throughout the high-speed leg on the tunnel structure and model.[5]

This current effort concentrated on reducing the tunnel structure dynamics in the lateral direction along the high-speed leg as a first step in reducing the dynamics.

Analysis of Tunnel Structural Response

The analysis of the fluctuating pressure data shows that the all the fluctuating pressures are broadband white noise without any specific frequencies and the level varies with the tunnel dynamic pressure. The model support area (arc sector and fixed fairing) experienced the largest fluctuating pressures of the entire high-speed leg.

This relationship between the fluctuating pressure and dynamic pressure is shown in figure 6 for the fixed fairing. The fixed fairing fluctuating pressures (p'_{FF-Y}) varies linearly with the tunnel dynamic pressure except for the exponential vertical spikes. These spikes occur when there is supersonic flow in the test section, and an unsteady normal shock exists in the arc sector/fixed fairing area causing a local increase in p'. Thus the tunnel can experience high fluctuating pressures even at very low dynamic pressures.

The analysis of the acceleration data indicated a similar relation between the local RMS accelerations ($\tilde{a}$) of a structural component and the dynamic pressure. Again, using the fixed fairing as an example, figure 7 shows the fixed

fairing RMS accelerations in the Y direction ($\tilde{a}_{FF\text{-}Y}$) along the centerline of the tunnel versus the dynamic pressure. This relation varies linearly except for the exponential vertical spikes associated with supersonic conditions.

The data for the fluctuating pressures and RMS accelerations were found to be mostly independent of temperature (and Reynolds No.). There is some indication that the high-speed diffuser response changes with pressure because of the increase in diffuser gas mass.

If one assumes a white noise (broadband) fluctuating pressure (p′) is acting on an exposed area of the structure (A), it will exert a force onto the structure. It can be theorized that the structure exposed to this force will then linearly respond at its natural modes. This relation can be simply expressed as:

NTF Simplified Structural Dynamics Model

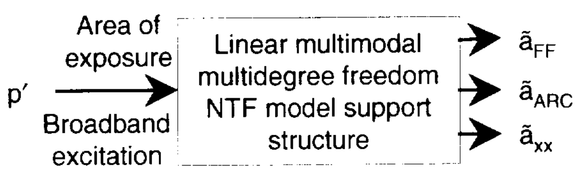

This simplified expression indicates that there is a relation between p′ and ã that is unique to each specific structural component and this relationship is characteristic of the component.

The data show a first order linear relation between the local fluctuating pressure (p′) and the local structural acceleration (ã) for all structural components. Again using the fixed fairing as an example, figure 8 shows this relation.

From figure 8 the slope ($\Delta\tilde{a}/\Delta p'$) provides a parameter that is a measurement of the inverse stiffness of the structure. This stiffness parameter can then be determined and compared for different structural components to identify areas of relative weakness. Table 1 provides a summary of the stiffness parameter for structures of the NTF high-speed leg from measured data.

Structure, Direction	Stiffness Parameter ($in/s^2/psi$)
Downstream Support Frame, Y	3,500
Model Support Frame, Y	5,300
Arc Sector Centerline, Y	22,000
Fixed Fairing Centerline, Y	60,000
High Speed Diffuser Lip, Z	240,000

Table 1 – NTF Structural Stiffness

This table shows that the most flexible and responsive structure is the high speed diffuser followed by the fixed fairing and arc sector. Surprisingly, the MSF and DSSF are only about 3-4 times stiffer laterally than the arc sector, when one can reasonably expect such support structure should be significantly stiffer.

Analysis of Model Response

The RMS values of six components of the model strain gauge balance (NF, SF, AF, PM, YM, RM) show a similar relation to the local fluctuating pressure (p'_{TS}). The analysis shows that the NF, SF, PM, and RM have a low response to p'_{TS}, and the YM and AF have a larger response. Figure 9 shows an example of this relation between the RMS value of the YM to p'_{TS}.

Frequency Domain Analysis

A frequency domain analysis was completed to identify the modes, and their characteristics, associated with different structures. As expected the amplitudes of each mode increased with increasing dynamic pressure as shown in figures 10 and 11.

Figure 10 shows the spectra of the arc sector center Y direction. The dominant mode frequencies are at 11-12Hz, 17-19Hz, 22-23Hz, 34-42Hz and 70+Hz. Although not the largest mode the 34-42Hz mode shows the characteristics of an aero-elastic mode where the frequency decreases from 42Hz to 34Hz as the dynamic pressure increases. In a detailed analysis it was determined that this mode changes frequency with dynamic pressure but does not show evidence of decreased damping. This mode behavior is explained by aerodynamic loading of the elastic arc sector.

Figure 11 shows the spectra of the fixed fairing center Y direction. The dominant mode frequencies are at 23Hz, 30-32Hz and at 70+Hz. The 30-32Hz mode is by far the most dominant frequency of the three modes. The smaller 23Hz

mode is an arc sector mode transmitting from the arc sector due to contact between the fixed fairing and arc sector.

Summary

The analysis provides an understanding of the dynamics problems at the NTF by first identifying and understanding the behavior of the local fluctuating pressures (p′) as the excitation source for the dynamics. The analysis also identified the relative stiffness of each structural component along the high-speed leg and, based on spectra analysis, identified the behavior and contributions of each structural component to dynamics.

Based on this analysis, the reduction of lateral dynamics response at the NTF can be accomplished by reducing p′ and/or increasing the stiffness of the model support structure in the load path.

SOLUTIONS

It was established early that any proposed solution could not change the tunnel flow lines; therefore any efforts to minimize p′ were not considered at this time.

From the data analysis it was clear that changes made in the model support structure (FF, Arc Sector, MSF and DSSF) were the best way to reduce the lateral dynamics. The solutions were divided into two areas:

1) Increase support structure stiffness
2) Change the structure boundary conditions

Increase Support Structure Stiffness

To increase the support structure stiffness (Arc Sector, MSF and DSSF), large 0.75in aluminum shear plates were installed horizontally securing together the MSF, outermost I-beams and DSSF. Additionally, bulkheads with extending lower brackets were installed between the top I-beams.[6]

Figures 12, 13, and 14 show simple graphical representations of the shear plates (upper and lower), bulkheads and brackets.

Change the Boundary Conditions

There were two solutions for changing the structure boundary conditions. One solution was to install wedges between the fixed fairing and the adjacent tunnel wall, and the second was the installation of new active bearings.

The fixed fairing wedges are designed to fill the gap between the fixed fairing and the tunnel floor. By filling this gap the wedges relocate the lateral support points of the fixed fairing from the vertical pin up to the tunnel floor. This change reduces the fixed fairing's effective length from 160in to 125in as shown in figure 15, thereby increasing its natural frequency and reducing its displacement.

The installation of new active bearings was based on the data analysis that indicated the top of the arc sector experienced large lateral accelerations and deflections. Additionally data from a previous report indicated tightening the existing bearings reduced the yaw dynamics of the model.[1] Therefore two pairs of active bearings (a front pair and an aft pair) were installed just above the existing bearings as shown in figure 15. These new active bearings can be remotely controlled to set up to 10000lbs load against the arc sector and still allow the arc sector to freely move. Operationally these new active bearings were loaded prior to tunnel operations and remained loaded at all times.

RESULTS

Installing the shear plates, brackets, bulkheads and the fixed faring wedges greatly reduced the dynamics of the tunnel model support area (MSF, DSSF, arc sector and fixed faring).

Figures 16 and 17 show the significant reduction in the stiffness parameter before and after the structural modifications for the fixed fairing and the arc sector. These results are summarized in Table 2 showing the increase in the tunnel model support structure stiffness.

Structure	Before Stiffness Parameter ($in/s^2/psi$)	After Stiffness Parameter ($in/s^2/psi$)
DSSF, Y	3500	200
MSF, Y	5300	470
ARC Centerline, Y	22,000	1300
FF Centerline, Y	60,000	3700

Table 2 –Structural Stiffness (Before and After)

The increased structural stiffness has resulted in a significant reduction of the amplitudes of the frequency spectra for each model support structure component. Figures 18 and 19 show this reduction for the fixed faring and arc sector.

For the fixed fairing spectra shown in figure 18 the previously dominating 30-32Hz mode has been significantly reduced and shifted to 45Hz.

In the arc sector spectra shown in figure 19 there remains four inherent modes at greatly reduced amplitudes. The first two modes around 8Hz and 12Hz are highly model/balance/sting dependent. The other two modes at 15-16Hz and 23Hz are associated with the model support structure and are inherent to the design of the arc sector.

With this significant decrease in the structural dynamics, there is also a small decrease in the model dynamics as shown in figure 20. This small reduction indicates, as expected, that the model dynamics are dominated by the model/balance/sting modes. Future work in reducing the model dynamics will be to avoid mode coalescence between the model/balance/sting and the modes inherent to the model support structure.

Active Bearings

The use of active bearings showed that the Y direction acceleration (and therefore displacement) at the top of arc sector was considerably reduced. However the Y direction accelerations of the centerline of the arc sector showed no discernable change. This suggests that the existing bearings are providing sufficient boundary conditions for the arc sector in their current configuration. The active bearings do however, provide a limited ability to move the frequencies of the arc sector modes. Further testing is required to fully document the results of using the active bearings.

FUTURE IMPROVEMENTS

Several efforts are currently underway to further reduce model dynamics. The NTF has finished fabrication of a new balance (NTF-116A) that is 4.3 times stiffer in pitch, 5.7 times stiffer in yaw and 12 times stiffer in roll without sacrificing data quality.[7] This balance should have significant impact in reducing model dynamics by avoiding coalescence with the modes inherent to the model support structure.

The NTF is also working to develop new stings using passive and active damping approaches to reduce the model dynamics and avoid any modal coalescence.

CONCLUSIONS

Providing additional stiffness to the model support structure has significantly reduced the problems of dynamics at the NTF. Efforts continue to further reduce the dynamics with future solutions focusing on reducing the model dynamics.

There will always remain some fundamental frequencies that are inherent to the support structure that cannot be eliminated. The design of future model/balance/stings system must avoid the frequencies of the support structure to prevent coalescence.

ACKNOWLEDGEMENT

The success of this work was made possible through the efforts of several groups working together for a common goal of improving the NTF. The authors would like to especially recognize T. Arboneaux, P. Bauer, J. Barry, J. Bledsoe M. Chambers, M. Hilleren, L. Rash, and J. Zalarick for their hard work.

REFERENCES

1. Young, C.; Popernack, T.; and Gloss, B.: National Transonic Facility Model and Model Support Vibration Problems, AIAA Paper No. 90-1416, 1990
2. Buehrle, R. D.; Young, C. P., Jr.; Balakrishna, S., and Kilgore, W. A.: Experimental Interactions Between Model Support Structure and High Speed Research Model in the National Transonic Facility, AIAA Paper No. 94-1623, 1994
3. Igoe, W. B.: Analysis of Fluctuating Static Pressure Measurements in the National Transonic Facility, NASA TP 3475, March 1996
4. Edwards, R. W.: National Transonic Facility Model and Tunnel Vibrations, AIAA Paper No. 97-0345, 1997
5. Balakrishna, S.: Data Analysis Report, NTF Operational Data from Tests 100, 107 and 111, Final Report – Part A, ViGYAN Report R00-05, NASA Langley Research Center, Contract NAS1-96014, Task RF01, February 2000
6. Butler, D. H.: NTF Structural Modification Proposal Based on NTF Operational Data Analysis, Final Report – Part B, ViGYAN Report R00-05, NASA Langley Research Center, Contract NAS1-96014, Task RF01, February 2000
7. Parker, P.: Cryogenic Balance Technology at the National Transonic Facility, AIAA Paper No. 2001-0758, 2001

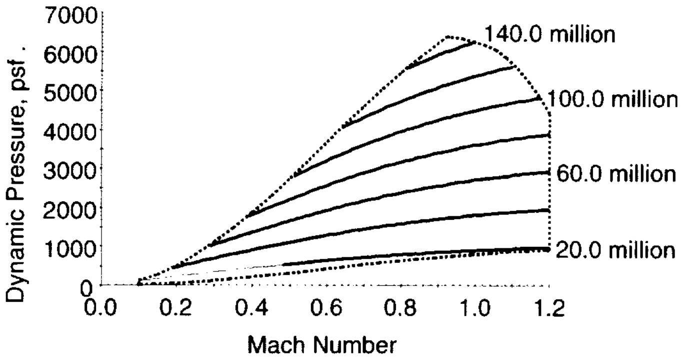

Figure 1 – NTF Operational Envelope

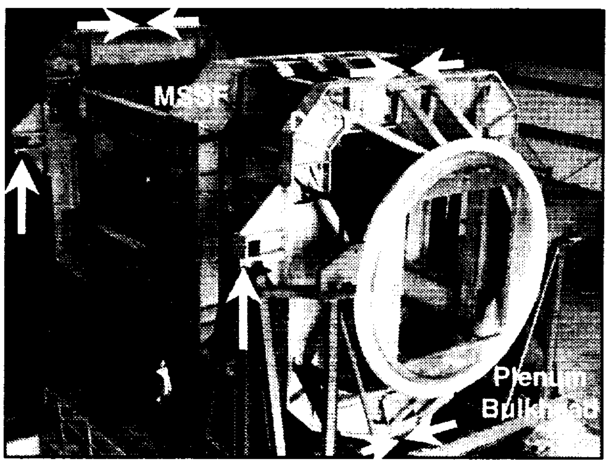

Figure 2 – Test Section Support Structure

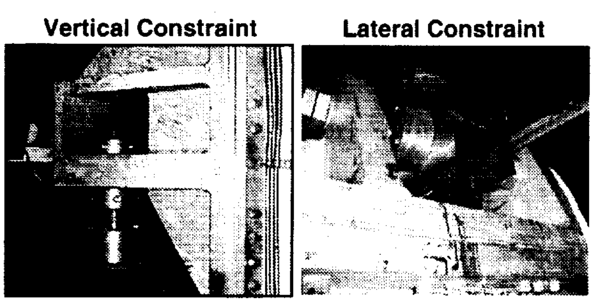

Figure 3 – Test Section Support Pads

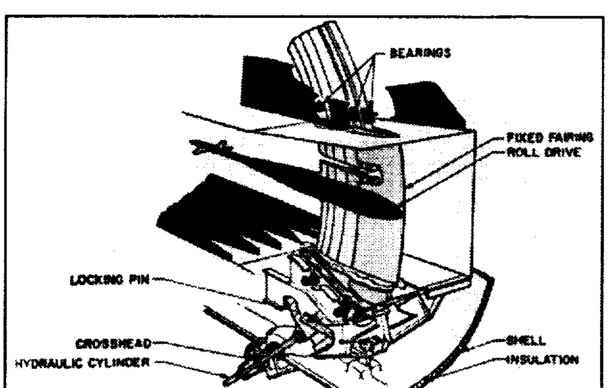

Figure 4 – Model Support Structure

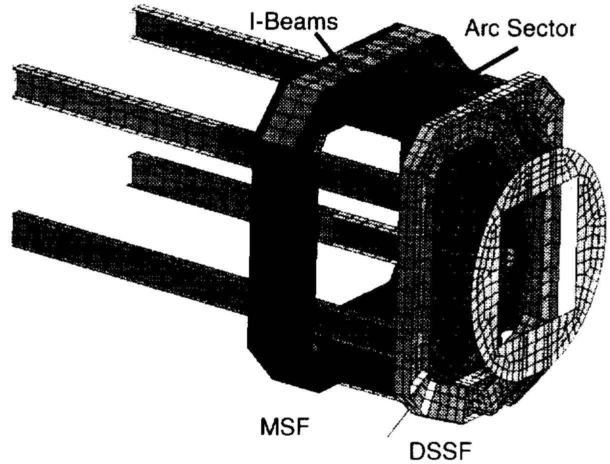

Figure 5 – Model Support Structure

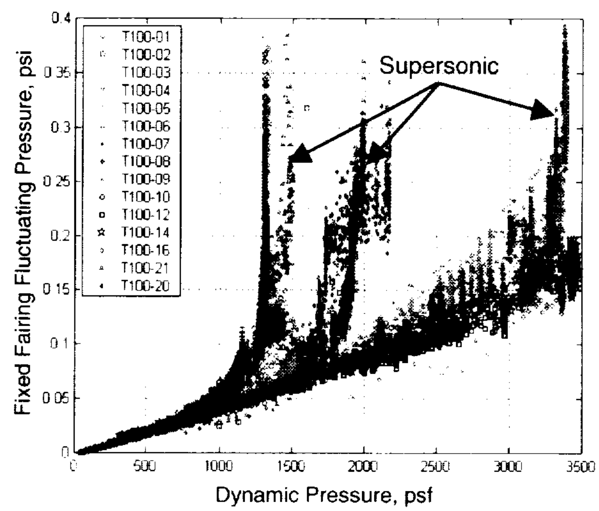

Figure 6 – Fixed Fairing Fluctuating Pressure vs. Dynamic Pressure

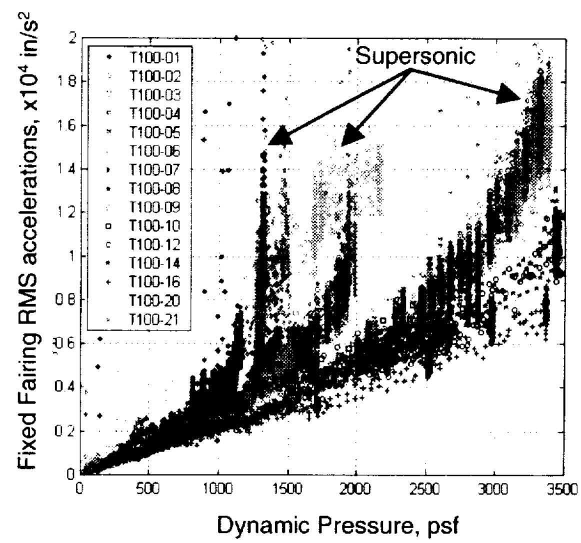

Figure 7 – Fixed Fairing RMS Acceleration vs. Dynamic Pressure

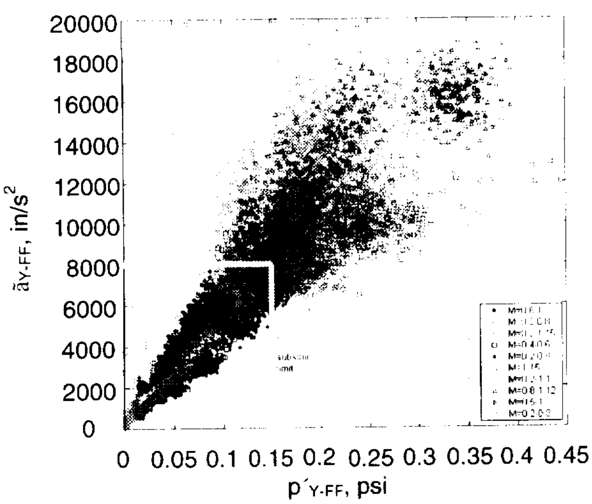

Figure 8 – Fixed Fairing RMS accelerations vs. Fluctuating Pressure

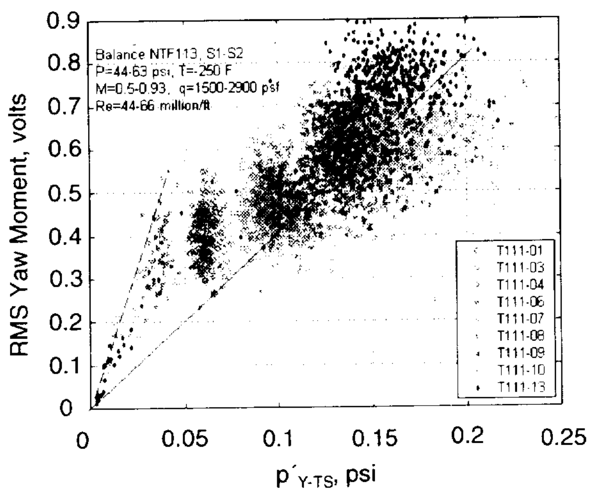

Figure 9 – RMS Yaw Moment vs. Fluctuating Pressure

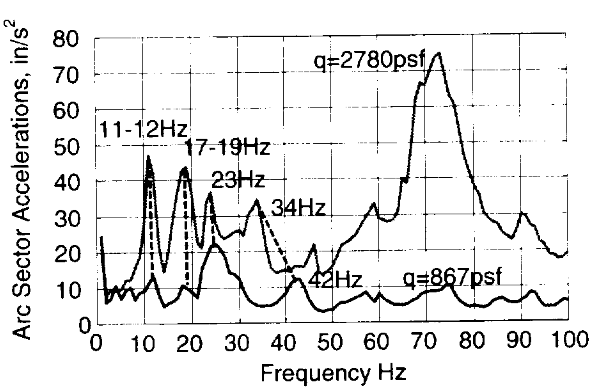

Figure 10 – Arc Sector Spectra for High and Low Dynamic Pressures

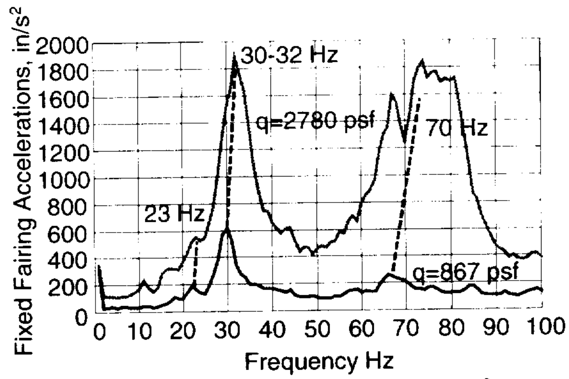

Figure 11 – Fixed Fairing Spectra for High and Low Dynamic Pressures

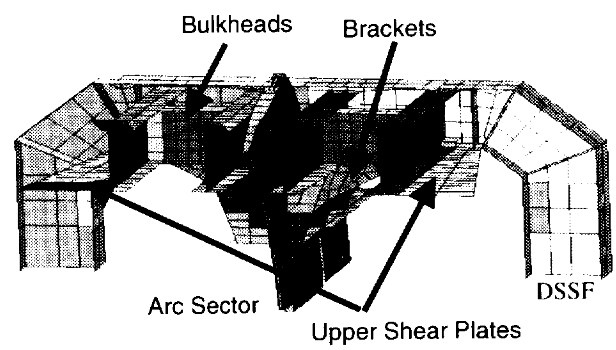

Figure 12 – Arc Sector/Support Structure (Top)

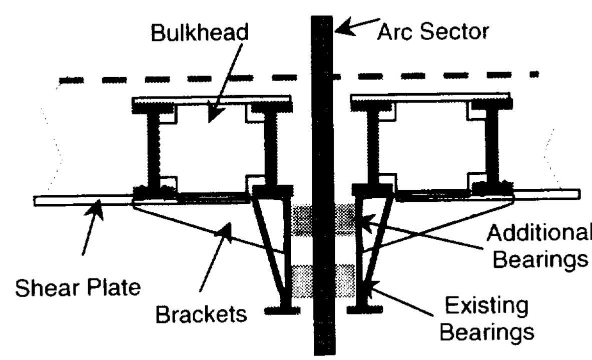

Figure 13 - Arc Sector/Support Structure (Top)

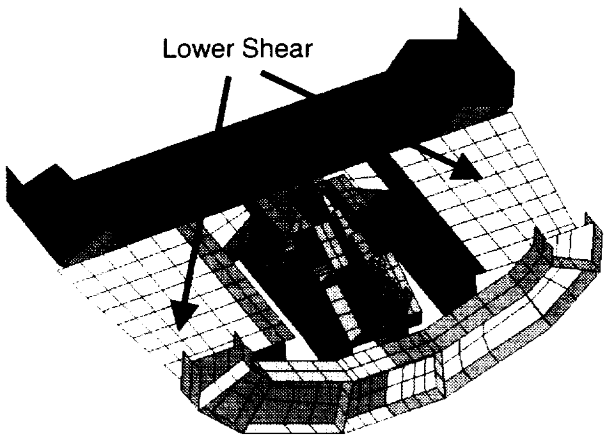

Figure 14 – Arc Sector/Support Structure (Bottom)

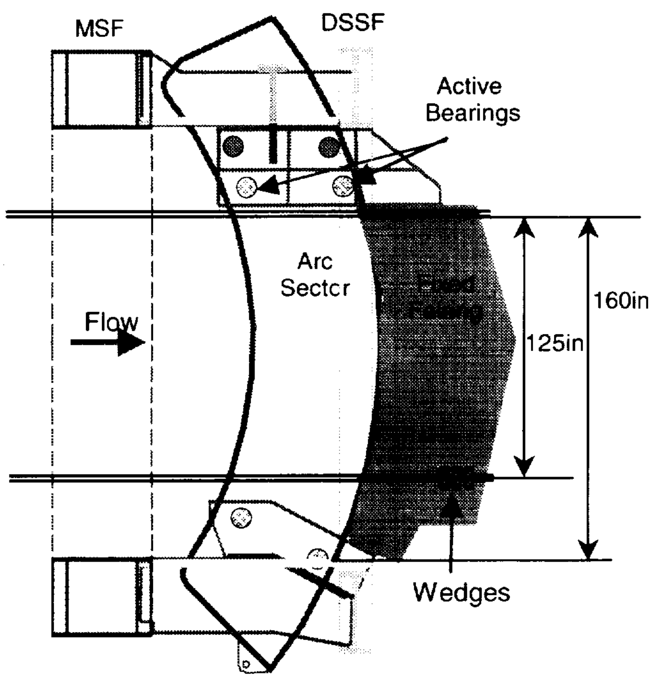

Figure 15 - Arc Sector/Support Structure (Sideview)

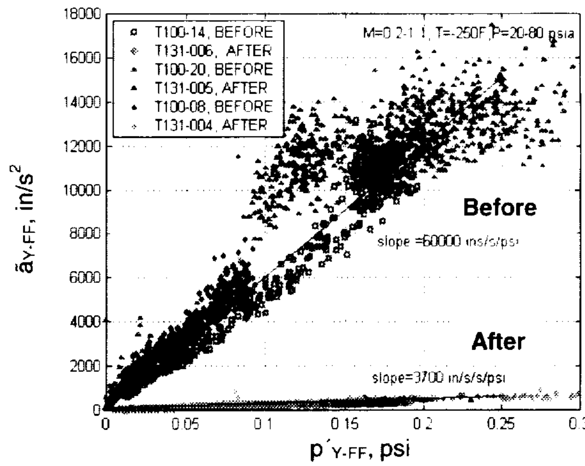

Figure 16 – Fixed Fairing Results (Before and After)

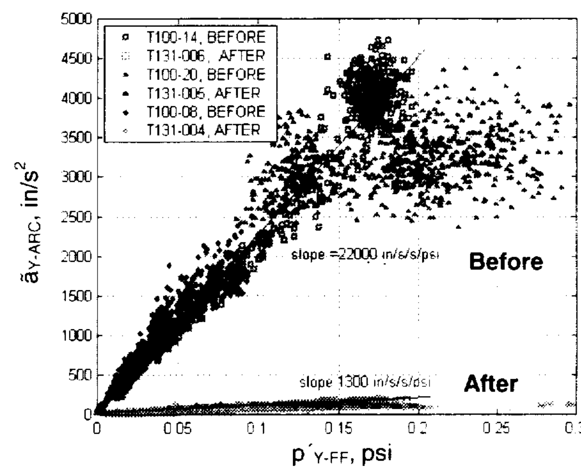

Figure 17 – Arc Sector Results (Before and After)

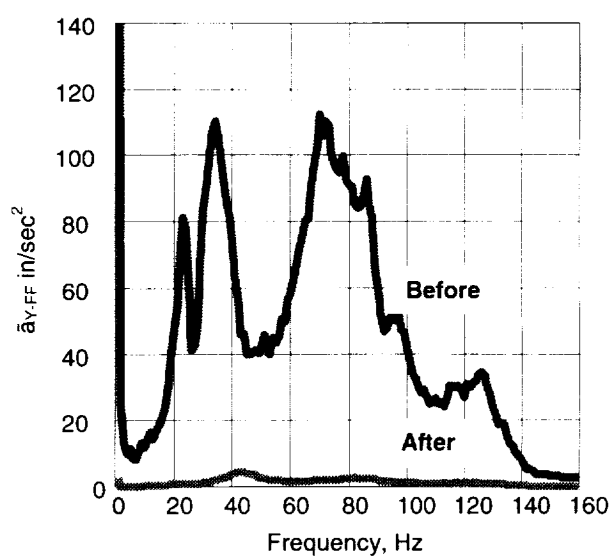

Figure 18 – Fixed Fairing Results (Before and After)

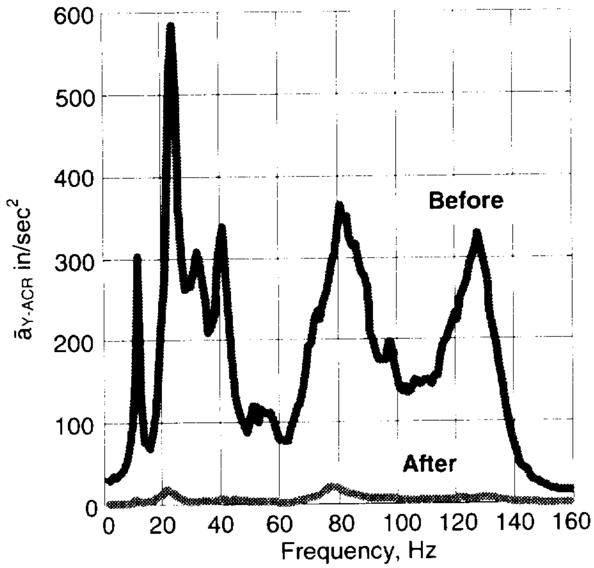

Figure 19 – Arc Sector Results (Before and After)

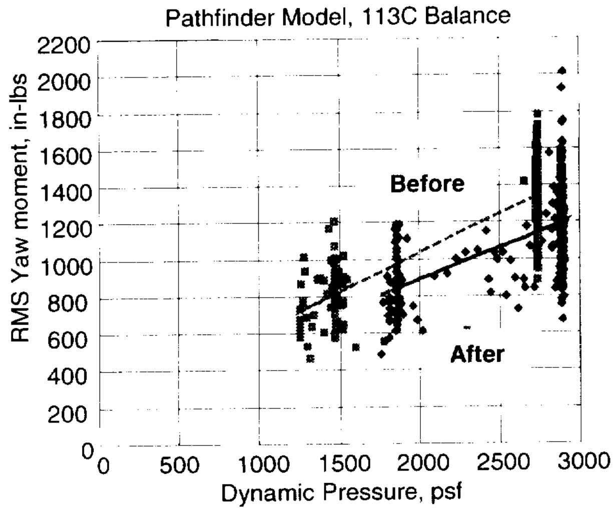

Figure 20 – Model Yaw Moment Results (Before and After)